



# Broadband, electro-optic, dual-comb spectrometer for linear and nonlinear measurements

DAVID R. CARLSON,<sup>1,2,\*</sup>  DANIEL D. HICKSTEIN,<sup>1</sup>  AND SCOTT B. PAPP<sup>1,2</sup> 

<sup>1</sup>*Time and Frequency Division, National Institute of Standards and Technology, 325 Broadway, Boulder, CO 80305, USA*

<sup>2</sup>*Department of Physics, University of Colorado, Boulder, CO 80309, USA*

\*[david.carlson@nist.gov](mailto:david.carlson@nist.gov)

**Abstract:** We demonstrate a dual-comb spectrometer based on electro-optic modulation of a continuous-wave laser at 10 GHz. The system simultaneously offers fast acquisition speed and ultrabroad spectral coverage, spanning 120 THz across the near infrared. Our spectrometer is highly adaptable, and we demonstrate absorption spectroscopy of atmospheric gases and a dual-comb configuration that captures nonlinear Raman spectra of semiconductor materials via coherent anti-Stokes Raman scattering. The ability to rapidly and simultaneously acquire broadband spectra with high frequency resolution and high sensitivity points to new possibilities for hyperspectral sensing in fields such as remote sensing, biological detection and imaging, and machine vision.

© 2020 Optical Society of America under the terms of the [OSA Open Access Publishing Agreement](#)

Dual-comb spectroscopy (DCS) can perform high-speed, high-spectral resolution, and high dynamic range measurements across large spectral bandwidths using two optical-frequency combs with slightly different repetition rates,  $f_{\text{rep}}$  [1,2]. Compared to other tools like grating-based or Fourier-transform spectrometers, DCS systems can offer unprecedented combinations of measurement speed and resolution, especially since DCS does not require physically movable components [3].

In DCS, broadband spectral data is collected in a sequence of time-domain interferograms that are captured with a photodetector, a high-speed, high-dynamic-range signal analyzer, and a high-capacity data-processing system. These interferograms repeat at the difference in repetition rate  $\Delta f_{\text{rep}}$  of the two frequency-comb sources, and thus their frequency spectrum contains a series of  $\Delta f_{\text{rep}}$  harmonics that correspond to the mode pairs from the optical combs. To avoid aliasing in the electronically detected spectrum, the maximum optical bandwidth  $\Delta\nu$  that can be captured in a single DCS measurement must satisfy

$$\Delta\nu \leq \frac{f_{\text{rep}}^2}{2\Delta f_{\text{rep}}}. \quad (1)$$

As a result, there are fundamental tradeoffs between acquisition rate ( $\Delta f_{\text{rep}}$ ), bandwidth ( $\Delta\nu$ ), and frequency point spacing ( $f_{\text{rep}}$ ) to consider when designing a DCS system. One approach to capturing large spectral bandwidths, at the expense of acquisition speed, is to utilize a small  $\Delta f_{\text{rep}}$  [4]. Alternatively, as we explore here, increasing the comb repetition rate allows the same optical bandwidth to be collected at faster rates and by processing and storing fewer data, though with reduced point spacing. Our approach is likely disfavored for characterizing narrow linewidth features of low-pressure gas samples, but it opens up a new tool to explore complex gas, liquid, and solid samples.

In this work, we present a DCS system based on electro-optic modulation (EOM) of a continuous-wave (CW) laser, realizing a new area of the DCS system configuration space

with regard to rapid measurement speed and wide spectral coverage. Our dual-EOM-comb spectrometer combines deterministic optical-pulse generation with optical-cavity filtering and spectral broadening in nonlinear nanophotonics to generate two 10-GHz-rate combs that cover a large portion of the near infrared. We use the system in two experimental configurations to perform proof-of-concept demonstrations of gas-phase absorption spectroscopy as well as nonlinear measurements of Raman spectra in solid-state materials through coherent anti-Stokes Raman scattering (CARS).

EOM frequency combs [5] are attractive for use in DCS systems due to the relative ease in maintaining mutual coherence between two combs that share the same pump laser and derive their repetition frequencies via phase-locked synthesis from a common electronic clock [6–9]. Since EOM combs are often created with a microwave-rate drive source in the  $\approx 1 - 30$  GHz range, they naturally support high-speed DCS acquisition and measurements [10]. However, EOM combs also present major challenges in implementing a DCS system at gigahertz rates, especially when spectral bandwidths of more than  $\approx 20$  THz are desired. In previous work, we showed how to overcome the limitations of low pulse energy and long pulse durations at these rates through supercontinuum generation in nonlinear fibers [11] and nonlinear waveguides based on silicon-nitride ( $\text{Si}_3\text{N}_4$ , henceforth SiN) [12]. Now, by seeding two different SiN waveguides with parallel 10 GHz EOM combs and overlapping the broadband outputs, our system can perform linear DCS across 120 THz (1000 nm) of simultaneous bandwidth and nonlinear CARS measurements across approximately  $600 \text{ cm}^{-1}$  of bandwidth.

The experimental setup for the base EOM comb is shown in Fig. 1, with further details provided in [12]. In brief, a 1550 nm CW laser, stabilized to an ultra-stable cavity for convenience, is used as the pump laser. The modulated output of the initial comb is transmitted through a Fabry-Perot filter cavity to suppress high-frequency thermal noise, and then compressed, amplified, and propagated through approximately 4 m of normal-dispersion highly nonlinear fiber. A free-space grating compressor provides fine-tuning of the pulse compression before seeding the SiN waveguide. The beam is coupled into the fundamental quasi-transverse-electric mode of the waveguide using an aspheric lens with  $\text{NA} = 0.6$ . Finally, the broadband output from the chip is collimated by an off-axis parabolic mirror for use in down-stream experiments.

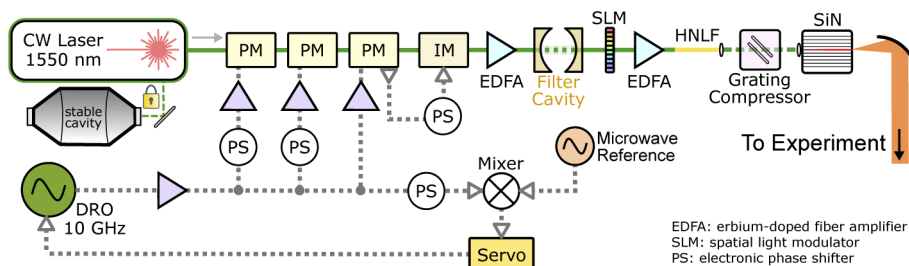


**Fig. 1.** Optical and electrical schematic of the EOM frequency comb system, including supercontinuum generation. A dielectric-resonator oscillator (DRO) produces a 10 GHz microwave signal, which drives the phase-modulators (PMs) and intensity modulator (IM) to convert the continuous-wave (CW) laser into a pulse train. A filter cavity removes high-frequency phase noise from the pulse train. Normal dispersion highly nonlinear fiber (HNLF) increases the bandwidth of the pulses, which are then compressed in a grating-based compressor before entering the silicon nitride (SiN) waveguide for supercontinuum generation. The wavelength of the CW laser is locked to an ultra-low expansion glass cavity, and the DRO is locked to a microwave reference.

For dual-comb operation, the setup in Fig. 1 is duplicated to create two, parallel systems. Mutual frequency and phase coherence between the combs is ensured through a shared CW

pump laser and a shared 10 GHz microwave oscillator; see Fig. 2(a). The difference in repetition rates between the combs is established by mixing  $\sim 100$  MHz signals, offset by  $\Delta f_{\text{rep}}$ , from two phase-locked channels of a synthesizer with the common 10 GHz oscillator. A 250 MHz acousto-optic modulator (AOM) is inserted into one of the comb arms to shift the interferogram carrier frequency away from baseband, thus avoiding signal aliasing [6].

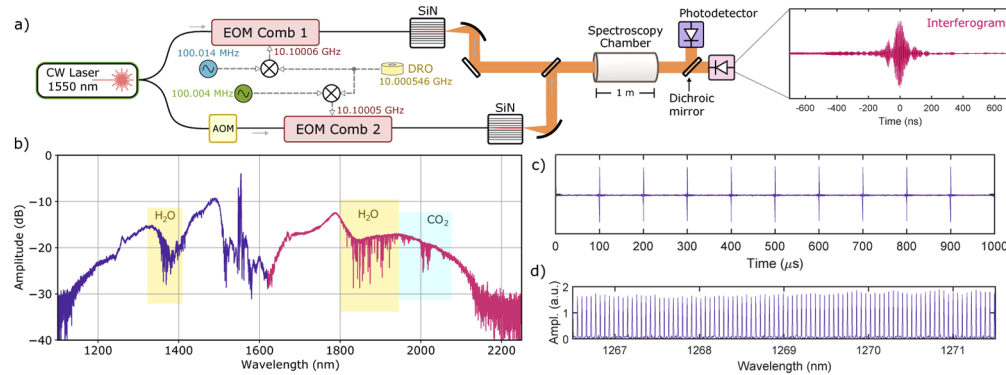


**Fig. 2.** a) Schematic for ultra-broadband linear dual-comb spectroscopy (DCS). Inset shows a sample DCS interferogram. b) Retrieved DCS spectrum showing gas-phase absorption features from  $\text{H}_2\text{O}$  and  $\text{CO}_2$  molecules. Spectrum obtained from a coherent average of 2000 interferograms at  $\Delta f_{\text{rep}} = 10$  kHz. c) Time-domain trace of multiple sequential interferograms. d) Frequency-domain spectrum of the interferogram sequence from c) showing fully resolved comb modes near a wavelength of 1270 nm.

In previous work, Baumann et al. showed that broadband DCS using the outputs of nonlinear SiN waveguides can produce spectra with signal-to-noise ratio (SNR) comparable to traditional fiber-based systems [13]. To make linear spectroscopy measurements with our EOM comb system, we adopt a similar approach and overlap the output of each SiN waveguide with identical polarizations on a broadband beam splitter. The combined beams are then transmitted through a 1 m long gas cell before collecting the interferograms. In principle, the interferograms can be recorded with a single photodetector, however to aid in our diagnostics, we use a dichroic splitter to divide the spectrum between two detectors at a cutoff wavelength of 1600 nm. With this configuration, we slightly improve the dynamic range of the short-wavelength detector by attenuating the 1560 nm region by approximately 10 dB using a free-space short-pass filter with a cutoff wavelength of 1500 nm. Figure 2(b) shows a sample broadband DCS output spectrum after transmission through the cell with approximately 1 atm  $\text{CO}_2$  at room temperature. The  $\text{CO}_2$  overtone vibration bands are clearly visible near 2000 nm, as well as two atmospheric  $\text{H}_2\text{O}$  bands from free-space propagation outside the chamber, highlighted in yellow.

The microwave frequencies and data sampling rates are all chosen to be integer multiples of  $\Delta f_{\text{rep}}$  to support coherent time-domain averaging of the interferogram traces [2]. Figure 2(c) shows a sequence of 11 interferograms, coherently averaged  $\sim 100$  times at  $\Delta f_{\text{rep}} = 10$  kHz. When Fourier transformed, this trace produces a comb-mode-resolved spectrum; see the expanded data near 1270 nm shown on a linear amplitude scale in Fig. 2(d). The spectral SNR of each 10 GHz comb mode in panel d is roughly  $2 \times 10^4 / \sqrt{5}$  of averaging time.

Figure 3 shows a sample spectroscopy measurement after transmission through 2 atm of pure  $\text{CO}_2$  at room temperature. A comb-tooth-resolved acquisition under similar conditions is shown in panel b) in comparison to a fitted reference model. The transmittance has been calculated by manually subtracting the background envelope of the recorded spectrum. In a more rigorous spectroscopy experiment, the secondary output port of the broadband beam splitter used to overlap the spectra could be used as a calibration Ref. [2]. Additionally, we note that optimization

of the SiN waveguide geometry can support DCS at wavelengths extending into the mid-infrared [13,14], where many spectroscopy targets of interest have absorption features.

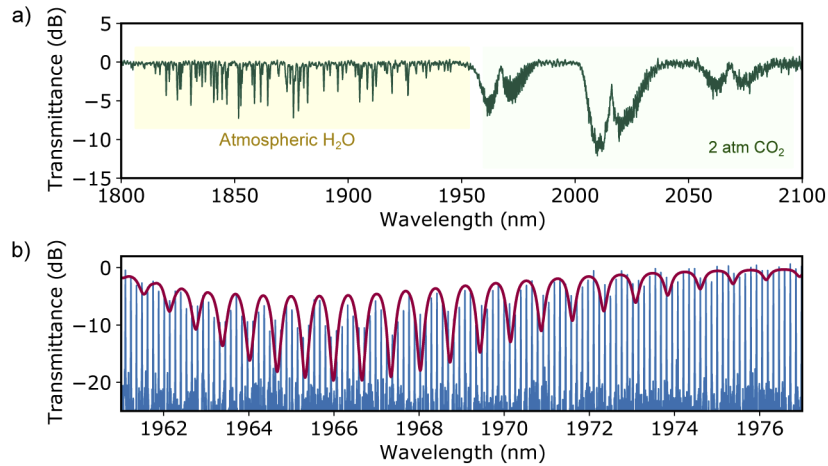


**Fig. 3.** a) Normalized transmittance spectrum in the 1800-2100 nm spectral range after transmission through the gas cell filled with 2 atm of CO<sub>2</sub>. b) Comb-resolved DCS spectrum (blue) of the CO<sub>2</sub> absorption bands near 1970 nm, with a fitted reference spectrum (red) overlaid for comparison.

Acquisition rates in the 10 kHz to 50 kHz range are readily achievable in our system, without aliasing. In principle, our 10 GHz system can support the same 120 THz (1000 nm) bandwidth at  $\Delta f_{\text{rep}}$  values up to approximately 400 kHz, with a suitable AOM frequency or via spectral division across two separate detectors.

In addition to broadband linear spectroscopy, our dual-EOM-comb system can be configured to produce broadband few-cycle pulses at the outputs of the SiN waveguides [12,15]. In this regime, the high peak intensities in sub-15-fs pulses can impulsively excite Raman vibrations in materials, and the dual-comb CARS technique [16–19] can be used to record Raman spectra. Our system implementation of dual-EO-comb CARS is shown schematically in Fig. 4(a). The overlapped output beams are focused into a test sample with a diffraction-limited 0.6 NA lens to an estimated intensity of  $5 \times 10^{10}$  W/cm<sup>2</sup>. A pair of long- and short-pass wavelength cutoff filters is then used to isolate light containing the CARS signal. A photodetector placed after the short-pass filter detects a sequence of interferograms, which are digitally recorded and Fourier transformed in post-processing to reveal the Raman response of the test sample.

To demonstrate this capability for dual-EO-comb CARS at  $f_{\text{rep}} = 10$  GHz, we focus the combs through a 380  $\mu\text{m}$ -thick crystalline Si wafer. Figure 4(c) shows a time-domain sequence of 20 sequential interferograms and the corresponding Fourier transform showing the characteristic 520  $\text{cm}^{-1}$  Raman peak with comb-resolved resolution and high signal-to-noise ratio. Alternatively, the Raman ring-down signal for a single interferogram (or average of several) can be captured directly with an oscilloscope and Fourier transformed to produce the spectrum shown in Fig. 4(f). Reasonable agreement between reference data [20] and the captured signal at 10 GHz is obtained.

The measurable bandwidth with this system is dependent on the spectral bandwidth and flatness of the comb, as well as the pulse compression quality of the seed lasers. The system demonstrated here addresses the 200  $\text{cm}^{-1}$  to 800  $\text{cm}^{-1}$  spectral range that is populated with molecular fingerprints. Indeed, we have carried out proof-of-concept measurements of several different crystalline material samples (Fig. 5), namely gallium arsenide, gallium phosphide, and silicon carbide. We expect that further optimization of the pulse compression [15] and focusing optics will immediately increase the applicable bandwidth and SNR by increasing peak

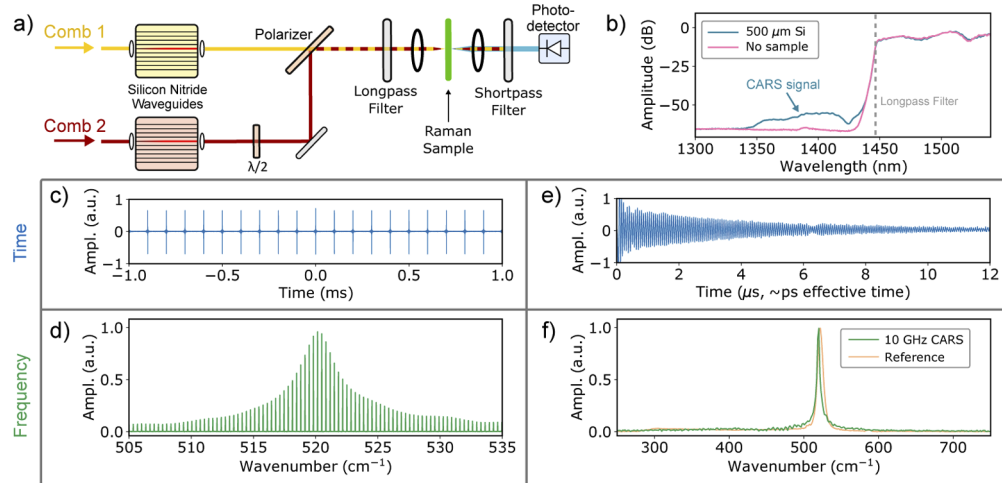


**Fig. 4.** a) Schematic for nonlinear dual-EOM-comb CARS. b) Optical spectrum near the longpass-filter band edge showing the CARS signal obtained after propagation through a 500  $\mu\text{m}$  thick silicon window. c) Time-domain interferogram sequence after optically isolating the CARS signal with a shortpass filter having a cutoff wavelength of 1400 nm. d) Fourier transform of the interferogram trace showing a comb-resolved Raman vibrational mode in silicon at 520  $\text{cm}^{-1}$ . e) Zoom of a single interferogram trace showing the Raman ringdown signal in the time domain. f) Comparison between reference data and a CARS spectrum obtained with the 10 GHz EOM comb.

intensities up to possibly five times higher in the focal volume. Still, such measurements of hard materials have intrinsic value in calibrating measurement systems and in the possibility of direct, hyperspectral microscopy of material samples.

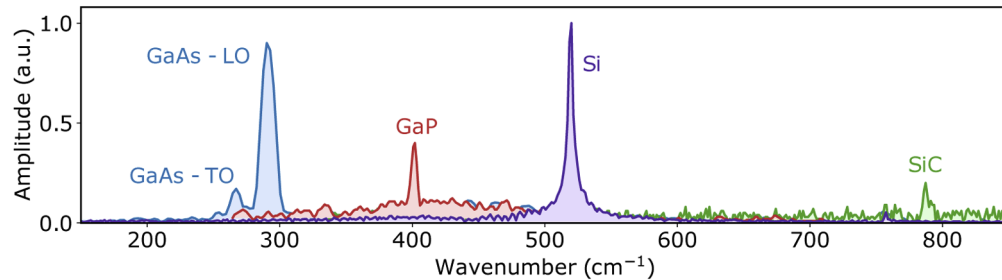


**Fig. 5.** Example Raman spectra acquired from various solid-state material samples with the 10 GHz dual-comb spectrometer. For GaAs, we observe both the longitudinal (LO) and transverse (TO) phonons.

While the peak power of our pulses is well suited for applications like biological or chemical imaging [21], the high average power of the 10 GHz comb sources ( $\sim 1$  W) makes beam or sample scanning critical to avoid physical damage. In our system, no scanning mechanism was implemented and liquid samples held in a cuvette tended to boil and form trapped bubbles in the focal region, unfortunately preventing any meaningful data acquisition. However, most potential applications of this ultra-high-speed CARS – such as real-time biological microscopy – require rapid scanning of the focal spot and would likely avoid this issue. Further, in a future series of experiments, it would be important to understand the inter-conversion rate of Raman scattering

for target samples and the optimum configuration to photodetect such a signal, especially for high repetition rate frequency combs [17].

The resolution of the dual-comb Raman spectrum is determined by the nominal comb repetition rate. In this case, we can achieve 10-GHz resolution, which is well-matched to many liquid- or solid-state Raman modes. While faster repetition rates could in principle further increase the acquisition speeds, the pulse energies quickly become too low to drive the nonlinear processes. Lower rate systems can readily provide high peak intensities, but the resolution is overly high and the speed too low for many specimens of biological interest. The amount of coherent averaging that can be supported in a given measurement should also be taken into account when determining the optimal repetition rate for a dual-comb CARS system. A more thorough investigation of these tradeoffs and their implications for measuring real-world samples may be the subject of future work.

The combination of high speed and broad spectral coverage in our system creates interesting possibilities for real-time measurement of fast transient events involving complex chemical profiles, such as combustion dynamics or in chaotic systems where long averaging is not possible due to their non-repeatable nature. We envision further refinements and simplifications to the experimental system, through additional integration and packaging, will lead to new measurement capabilities with dual-comb sources.

## Funding

Jet Propulsion Laboratory; Defense Advanced Research Projects Agency; National Institute of Standards and Technology.

## Acknowledgment

We thank Greg Rieker for providing the spectroscopy chamber, and Charles Camp Jr., Marcus Cicerone, Scott Diddams, Nazanin Hoghooghi, and Pablo Acedo for thoughtful comments, advice, and assistance on the work.

## Disclosures

DDH is currently employed by KMLabs Inc., a company that manufactures femtosecond lasers. DRC is a co-founder of Octave Photonics, a company specializing in nonlinear integrated photonics.

## References

1. S. Schiller, "Spectrometry with frequency combs," *Opt. Lett.* **27**(9), 766–768 (2002).
2. I. Coddington, W. Swann, and N. Newbury, "Coherent Multiheterodyne Spectroscopy Using Stabilized Optical Frequency Combs," *Phys. Rev. Lett.* **100**(1), 013902 (2008).
3. I. Coddington, N. Newbury, and W. Swann, "Dual-comb spectroscopy," *Optica* **3**(4), 414 (2016).
4. S. Okubo, K. Iwakuni, H. Inaba, K. Hosaka, A. Onae, H. Sasada, and F.-L. Hong, "Ultra-broadband dual-comb spectroscopy across 1.0–1.9  $\mu\text{m}$ ," *Appl. Phys. Express* **8**(8), 082402 (2015).
5. A. Parriaux, K. Hammani, and G. Millot, "Electro-optic frequency combs," *Adv. Opt. Photonics* **12**(1), 223 (2020).
6. G. Millot, S. Pitois, M. Yan, T. Hovhannisyanyan, A. Bendahmane, T. W. Hänsch, and N. Picqué, "Frequency-agile dual-comb spectroscopy," *Nat. Photonics* **10**(1), 27–30 (2016).
7. B. Jerez, P. Martín-Mateos, F. Walla, C. de Dios, and P. Acedo, "Flexible Electro-Optic, Single-Crystal Difference Frequency Generation Architecture for Ultrafast Mid-Infrared Dual-Comb Spectroscopy," *ACS Photonics* **5**(6), 2348–2353 (2018).
8. A. J. Fleisher, D. A. Long, Z. D. Reed, J. T. Hodges, and D. F. Plusquellic, "Coherent cavity-enhanced dual-comb spectroscopy," *Opt. Express* **24**(10), 10424 (2016).
9. A. Parriaux, K. Hammani, and G. Millot, "Two-micron all-fibered dual-comb spectrometer based on electro-optic modulators and wavelength conversion," *Commun. Phys.* **1**(1), 17 (2018).
10. V. Durán, S. Tainta, and V. Torres-Company, "Ultrafast electrooptic dual-comb interferometry," *Opt. Express* **23**(23), 30557 (2015).

11. K. Beha, D. C. Cole, P. Del'Haye, A. Coillet, S. A. Diddams, and S. B. Papp, "Electronic synthesis of light," *Optica* **4**(4), 406 (2017).
12. D. R. Carlson, D. D. Hickstein, W. Zhang, A. J. Metcalf, F. Quinlan, S. A. Diddams, and S. B. Papp, "Ultrafast electro-optic light with subcycle control," *Science* **361**(6409), 1358–1363 (2018).
13. E. Baumann, E. V. Hoenig, E. F. Perez, G. M. Colacion, F. R. Giorgetta, K. C. Cossel, G. Ycas, D. R. Carlson, D. D. Hickstein, K. Srinivasan, S. B. Papp, N. R. Newbury, and I. Coddington, "Dual-comb spectroscopy with tailored spectral broadening in Si<sub>3</sub>N<sub>4</sub> nanophotonics," *Opt. Express* **27**(8), 11869 (2019).
14. H. Guo, W. Weng, J. Liu, F. Yang, W. Hansel, C. S. Bres, L. Thevenaz, R. Holzwarth, and T. J. Kippenberg, "Nanophotonic supercontinuum based mid-infrared dual-comb spectroscopy," arXiv:1908.00871 (2019).
15. D. R. Carlson, P. Hutchison, D. D. Hickstein, and S. B. Papp, "Generating few-cycle pulses with integrated nonlinear photonics," *Opt. Express* **27**(26), 37374 (2019).
16. T. Ideguchi, S. Holzner, B. Bernhardt, G. Guelachvili, N. Picqué, and T. W. Hänsch, "Coherent Raman spectro-imaging with laser frequency combs," *Nature* **502**(7471), 355–358 (2013).
17. K. J. Mohler, B. J. Bohn, M. Yan, G. Mélen, T. W. Hänsch, and N. Picqué, "Dual-comb coherent Raman spectroscopy with lasers of 1-GHz pulse repetition frequency," *Opt. Lett.* **42**(2), 318 (2017).
18. N. Coluccelli, C. R. Howle, K. McEwan, Y. Wang, T. T. Fernandez, A. Gambetta, P. Laporta, and G. Galzerano, "Fiber-format dual-comb coherent Raman spectrometer," *Opt. Lett.* **42**(22), 4683 (2017).
19. T. Ideguchi, T. Nakamura, S. Takizawa, M. Tamamitsu, S. Lee, K. Hiramatsu, V. Ramaiah-Badarla, J.-w. Park, Y. Kasai, T. Hayakawa, S. Sakuma, F. Arai, and K. Goda, "Microfluidic single-particle chemical analyzer with dual-comb coherent Raman spectroscopy," *Opt. Lett.* **43**(16), 4057 (2018).
20. B. Lafuente, R. T. Downs, H. Yang, and N. Stone, "The power of databases: the RRUFF project," in *Highlights in Mineralogical Crystallography*, (De Gruyter, Berlin, Germany, 2016), pp. 1–30.
21. C. H. Camp Jr and M. T. Cicerone, "Chemically sensitive bioimaging with coherent Raman scattering," *Nat. Photonics* **9**(5), 295–305 (2015).